33rd Electric Vehicle Symposium (EVS33)
Portland, Oregon, USA, June 14 - 17, 2020

High Voltage Supercapacitor with Asymstric Graphene Nanowall Electrodes

Kun-Ping Huang[1], Yu-Wen Chi[1], Da-Je Hsu[2], Meng-yu Tsai[3], Su-Chih Hsu[3], Ming-Hui Hu[3], Chung-Hao Hsu[3], Zuo-Jhang Wu[3], Ying-Jhih Jhou[3], Chi-Chang Hu[2]

1Mechanical and Mechatronics Systems Research Laboratories, Industrial Technology Research Institute, 195, Sec. 4, Chung Hsing Road, Chutung, Hsin-Chu 31040, Taiwan, R.O.C., kphuang@itri.org.tw

[2] Department of Chemical Engineering, National Tsing Hua University, 101, Section 2, Kuang-Fu Road, Hsin-Chu 30013, Taiwan, R.O.C.

[3]Department of Air Quality Protection and Noise Control, Environmental Protection Administration, Executive Yuan, R.O.C., 14F, No.4, Xiushan St.,Taipei City 10042, Taiwan, R.O.C.

Summary

The plasma-enchanced chemical vapor deposition (PECVD) tool was used to grow graphene nanowalls (GNWs) and nitrogen-doped graphene nanowalls (NGNWs) on titanium substrate. Two identical GNW/ Ti electrodes were assembled in asymmetric electrical double layer capacitors (EDLC). Meanwhile, the asymmetric EDLC consisted of a positive GNW/Ti electrode and a negative NGNW/Ti electrode. The binder-free, vertically grown GNW and NGNW electrodes respectively provided good examples for extending the upper potential limit of a positive electrode of EDLCs from 0.1 to 1.5 V (vs Ag/AgNO3) as well as the lower potential limit of a negative electrode of EDLCs from −2.0 V to ca. −2.5 V in 1 M tetraethylammonium tetrafluoroborate/propylene carbonate ($TEABF_4$)/ propylene carbonate (PC) compared to activated carbons. This designed asymmetric EDLC exhibits a cell voltage of 4 V, specific energy of 30 Wh kg^{-1}, and specific power of 4 kW kg^{-1} and ca. >92% coulombic efficiency after 10,000 charge/discharge cycles, reducing the number of EDLC connections for a larger module voltage application. This work brings up the future where we can combine EDLCs and LIBs in advanced applications.

Keywords: Electrical double layer capacitor, Electrode, Energy Density, Power Density, Supercapacitor

1 Introduction

Electric vehicles (EVs) have received wide attention in recent years due to the huge contribution of conventional vehicles to carbon dioxide emission worldwide [1]. Currently EVs use lithium ion batterys (LIBs) as their power source. Supercapacitors (SCs), also known as electrochemical capacitors, are an important type of energy storage devices with great application potential. In comparison with most rechargeable batteries, SCs possess the unique characteristics such as high power density, fast charge-discharge rate capability, and long cycle life [2-4]. The dielectric capacitors exhibit a high power density but their energy density is extremely low. In contrast, batteries and fuel cells generally possess high energy

densities but low power performances. Engineers are committed to find a desirable energy storage device that can fill this gap and, fortunately, supercapacitors meet this requirement [5], making them become highly attractive in the past decades. If SCs can combine with LIBs, SCs can help to cover high power output and input for EVs. In addition, SCs also can stablize the power supply system which can extend the LIB life of EVs.

Graphene is a monatomic layer plane separated from graphite. In 2004, Geim and Novoselov successfully obtained monolayered graphene using the tape-mechanical stripping method [6], opening the worldwide interest in graphene researches although Kohlschütter and Haenni described the graphite oxide paper in 1918 [7] and Ruess and Vogt published the earliest transmission electron microscopic (TEM) images of few-layer graphene (layers of graphene between 3 and 10 layers) in 1948 [8]. Moreover, many researches have demonstrated that graphene is an ideal material for the SC electrodes because of its high theoretical surface area ($2630 m^2 g^{-1}$) and good electrical conductivity [9-12]. Graphene can be generally synthesized by the top-down and bottom-up methods [13]. The top-down methods include the exfoliation of graphite (starting material) through mechanical (e.g., Scotch tape [14]), chemical (e.g., solution-based exfoliation [15]), or electrochemical (oxidation/reduction and exfoliation [16-20]) processes, aiming at diminishing the van der Waals forces between graphene layers.

Graphene nanowalls (GNWs) are vertically-oriented graphene sheets. GNW has been successfully synthesized in different experimental conditions on metal foils in the reactive hydrocarbon gases and inar gases using a capacitively coupled plasma-enchanced chemical vapor deposition [21]. Graphene is a two dimensional structure composed of a single layer. GNW presents a number of unique properties, such as large specific surface area, long and thin edges, three-dimensional network morphology, good electrical property as well as structural stability [22–25]. These features make GNW promising for applications in supercapacitors [26].The traditional electrode of supercapacitor uses active carbon as active material. It needs to mix binding and conductive additives. These additive materials will react with supercapacitor electrolyte at higher voltage (>3V). GNW can be grown on electrode substrate which serves as the electrode material of supercapacitor directly. GNW does not react with the electrolyte, so it has higher potential to make high voltage supercapacitor [27-31].

In this work, we use the plasma-enhanced chemical vapor deposition (PECVD) tool (figure 1) for preparing vertically grown, few-layer GNW on titanium substrates. The intrinsic merits of such vertically grown GNW include: (1) GNW without adding binders or other additives show the high chemical stability; (2) the as-prepared GNW are of very high purity; and (3) this method takes few minutes to produce a piece of GNW [29, 31]. Such GNWs with high graphene purity and chemical stability exhibit a stable and wide potential window in the organic electrolyte [29, 31], which is suitable for electrochemical intercalation of ions in the highly positive or negative potential regions. The purpose of this work is to investigate the parameters of CV activation to enhance the specific capacitance and enlarge the working potential windows of few-layer GNW in commercially available organic electrolytes to promote the energy density of graphene-based SC from $E = CV^2/2$ where E, C, and V are respectively indicative of energy density, specific capacitance and cell voltage [32]. Several parameters of CV activation, such as potential window, cycle number, activation time, etc., will be investigated to optimize the capacitive performance of GNW. The cell voltage of activated graphene-based EDLCs in 1M $TEABF_4$/PC can be extended to ca. 3.8-4V with a relatively higher specific energy.

2 Experiment

2.1 Synthesis of GNW and NGNW

All GNWs were synthesized by plasma-enhanced chemical vapor deposition (PECVD) method. The design of process tool is shown in figure 1. The argon gas was excited with background plasma using 2.45 GHz microwave in the PECVD tool to directly grow vertical GNW onto Ti current collectors without any binders. Methane (CH_4) with a flow rate of 20−40 mL min^{-1} mixed with argon (Ar) in a volume ratio varying from 20 to 100% was fed into the reaction chamber. The microwave power was set between 500 and 1500 W for 10 min under a pressure from 20 mTorr to 760 Torr. NGNWs were directly grown onto Ti substrates by the PECVD method using a mixed flow of CH_4 and nitrogen ($N_{2)}$ with a total flow rate of 40 mL min^{-1} and CH_4/N_2 volume ratio = 1. The microwave power was set at 1000W for 10 min under a pressure of 40 mTorr. Figure

2.2 Electrochemical activation

All the electrochemical measurements and electrolyte preparation were conducted in a glove box (mBrum, Germany) with oxygen and water < 0.5 ppm. Cyclic voltammetry (CV) was employed to electrochemically activate GNWs in 1M $TEABF_4$/PC to enhance their specific capacitances under a three-electrode mode where GNWs, Ag/ $AgNO_3$, and activated carbon are employed as the working, reference, and counter electrodes, respectively. The upper and lower potential limits of CV, activation time, and activation potential window are the variables for optimizing the capacitance performance. The specific capacitance of GNWs before and after activation was normally evaluated by CV in specified potential windows.

2.3 Characterization

In this study, Graphene morphology was characterized by performing in an 80kV Cs-corrected TEM (JEOL, JEM-ARM-200F) and STEM-EELS analysis were applied to characterize the K-edge absorption of carbon. The energy resolution measured by the full width at half maximum of a zero-loss peak was about 0.4 eV through a cold field emission gun. The copper grid was cleaned by Ar/H_2 plasma before sample preparation in order to increase hydrophilicity and reduce contamination. X-ray photoelectron spectroscopy (XPS) analysis was performed using a Thermo VG ESCALAB250 spectrometer with an Al Kα (hv = 1486.69 eV) X-ray source. Raman spectra were determined by micro-Raman analysis (Thermo DXR HR Raman Microscope, HORIBA) using a 532 nm laser. The grazing incident diffraction (GID) patterns were detected by an X-Ray powder diffractometer (Rigaku_TTRAX Ⅲ, Japan). The electrochemical activation and capacitance evaluation were measured by an electrochemical analyzer (CHI760E, USA).

3 Results and discussion

3.1 Materials Characterization

Material characteristics of GNW and NGNW examined by means of Raman and XPS analyses as well as SEM (scanning electron microscope) cross-section and STEM images are shown in Figure 2. The cross section image of NGNWs in Figure 2(a) displays a continuous and vertical architecture with total thickness of 42.69 μm. The STEM image in Figure 2(b) reveals good quality of NGNW with the film thickness of ca. 1 nm (i.e., 2−3 layers). From curve 1 in Figure 2(c), the XPS spectrum of NGNW indicates an implanted nitrogen content of 7.6 at. % and the presence of a few oxygencontaining functional groups. The depth-profile XPS results (every 30 s, argon plasma etching with one XPS measurement) reveal the uniform distribution of N atoms doped onto the 3D NGNWs. Figure 2(d) displays a good lattice arrangement of NGNWs from the sharp 2D band and G band peaks. The high D band intensity of NGNWs indicates a relatively higher defect density because nitrogen doping significantly reduces the graphene domain size. In addition, the carbon defects formed by nitrogen doping can react with oxygen molecules in the air, leading to the presence of oxygen functional groups. Despite the very little knowledge about the heteroatom doping during the vertical growth of graphene, this work demonstrates an efficient, one-step method for growing the vertical nitrogen-doped graphene with the nitrogen content reaching 7.6 at. % and a few oxygen (< 2 at. %). The amount of sp^2-bonding of GNWs and NGNWs can be ascertained by the ratio between π^* bonding and $\pi^* + \sigma^*$ bonding through the electron energy loss spectroscopy (EELS, see Figure 2(e)) [33, 34]. The C_{60} has 100% sp^2-bonding which was used as the standandard sample. GNWs and NGNWs have 97% and 90% sp^2-bonding respectively. The nitride carbon bond can form pyrrolic N bonding introducing sp^3-bonding into graphene [35]. It results in sp^2-bonding decreasing.

3.2 CV activation of GNW

From the literature [36], anions will be intercalated into the graphite layers, resulting in the expansion of the interlayer space and increment of the specific capacitance, when a relatively positive electrode potential is applied to the graphite materials. In addition, the charge and discharge cycles in the expanded graphite might be reversed after the first irreversible charge process. The irreversible intercalation characteristic of anions into GNWs is also visible in Fig. 3(a) where GNWs were scanned between 0 and 2 V in 1M $TEABF_4$/PC (vs. Ag/AgNO3) for 10 cycles. From the first positive scan, the voltammetric current density rises sharply from ca. 1.5-2 V, suggesting that the onset of anion intercalation commences at 1.5 V. After the first cycle, the

voltammetric current density decreases gradually till a steady-state value. A comparison of two CV curves in Fig. 3(b) reveals that the voltammetric current density of GNWs is obviously enhanced by CV activation, indicating that the CV activation is feasible to improve the utilization of GNWs. Although a minor irreversible reduction peak is visible at electrode potentials close to -2 V for the activated GNWs, it decreases gradually along with the increment of scanning cycles. From all the above results and discussion, anions can be intercalated into GNWs (few-layer graphene) in the highly positive potential region (>ca.1.3 V), which can be used to electrochemically activate GNWs for promoting the specific capacitance of GNWs. Due to the unique structure of GNW, an incident angle of low angle XRD (also called grazing incident diffraction, GID), smaller than 5°, was employed to detect the characteristic (002) peak of graphene (see Fig. 4). The scan rate is 1 ° min^{-1}, from 5 to 80 °. From pattern 1 in Fig. 4 for the as-prepared GNW sample before CV activation, the GID pattern shows a small and broad peak at ca. 25 °, indicating the few-layer graphene structure. The other diffraction peaks around 35-45 ° on this pattern correspond to the Ti substrate. After the CV activation (see pattern 2), the (002) peak completely disappears, presumably attributed to the irregular expansion of the interlayer distance caused by residual ions intercalated into the few-layer structure.

3.3 Asymmetric Supercapacitor

The results of electrochemical tests of this asymmetric supercapacitor (ASC) are shown in Fig. 5. Fig. 5(a) is the CV curve with a high cell voltage of 4 V at 25mV s^{-1} in 1M $TEABF_4$/PC, showing a very rectangular shape, indicating good SC performance. The peak around 4 V due to the irreversible reaction(s) on positive and/or negative electrodes gradually decreases with increasing the cycles without sacrificing the coulombic efficiency. Fig. 5(b) shows the charge/discharge curve of this ASC at a cell voltage of 4 V and a current density of 1 A g^{-1} (based on the total active materials of both electrodes. This curve shows a highly symmetric triangle shape, representing excellent reversibility. Fig. 5(c) demonstrates the cycling stability of this ASC for 10,000 cycles at 4 V in 1M $TEABF_4$/PC. Note that after 10,000 charge/discharge cycles, the cell capacitance is about 108% of the capacitance value obtained from the first cycle. This result is attributable to the minor electrochemical activation of GNWs and NGNWs on both positive and negative electrodes at a cell voltage of 4 V. Since the cycle stability test was conducted at 4 V, this test is expected to exhibit a minor effect of electrochemical activation. Accordingly, about 8% increase in the cell capacitance and relatively low coulombic efficiencies (between 92 and 97%) were obtained in this 10,000-cycle test for this full cell. Since the coulombic efficiency is always higher than 90% for the above 10,000-cycle stability test, the charge storage reversibility of this ASC at a cell voltage of 4 V seems to be acceptable. Although specific capacitance ($C_{S,T}$) of GNWs after CV activation is not very high, this ASC exhibits a specific energy of 30 $Whkg^{-1}$ at a specific power of 4 $kWkg^{-1}$ on the basis of the total mass of electrode materials.

4 Conclusion

Cyclic voltammetry in highly positive and negative potential ranges has been demonstrated to be an effective activation method to significantly enhance the specific capacitance ($C_{S,T}$) of graphene nanowalls (GNWs) in 1M $TEABF_4$/PC. Anions and cations can be reversibly intercalated/de-intercalated into/from the graphene layers, improving the utilization of GNWs although some residual electrolytes should be left within the activated GNWs. Electrode potential and activation time are two main factors determining the capacitance enhancement of GNWs while the upper and lower potential limits of CV activation are respectively equal to +2.0 and -3.0 V (vs. $Ag/AgNO_3$). The charge storage reversibility and stability of GNWs after CV activation are good for constructing an ASC operated at a cell voltage of 4 V although CS,T of GNWs after CV activation is not very high. This ASC exhibits the specific energy of 30 Wh kg^{-1} at the specific power of 4 $kWkg^{-1}$, showing another advantage.

5 Figures

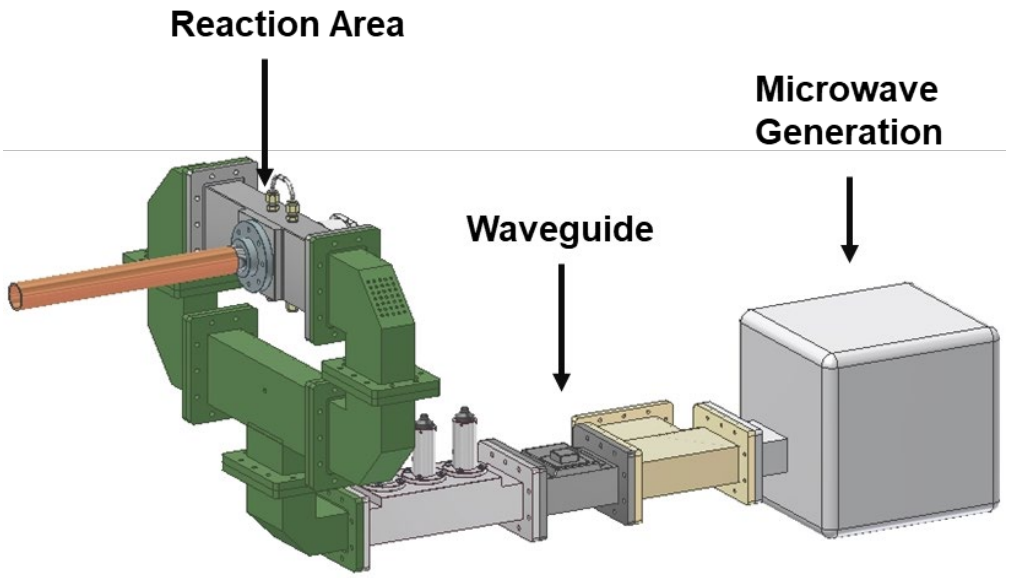

Figure 1. The design figure of microwave plasma torch tool

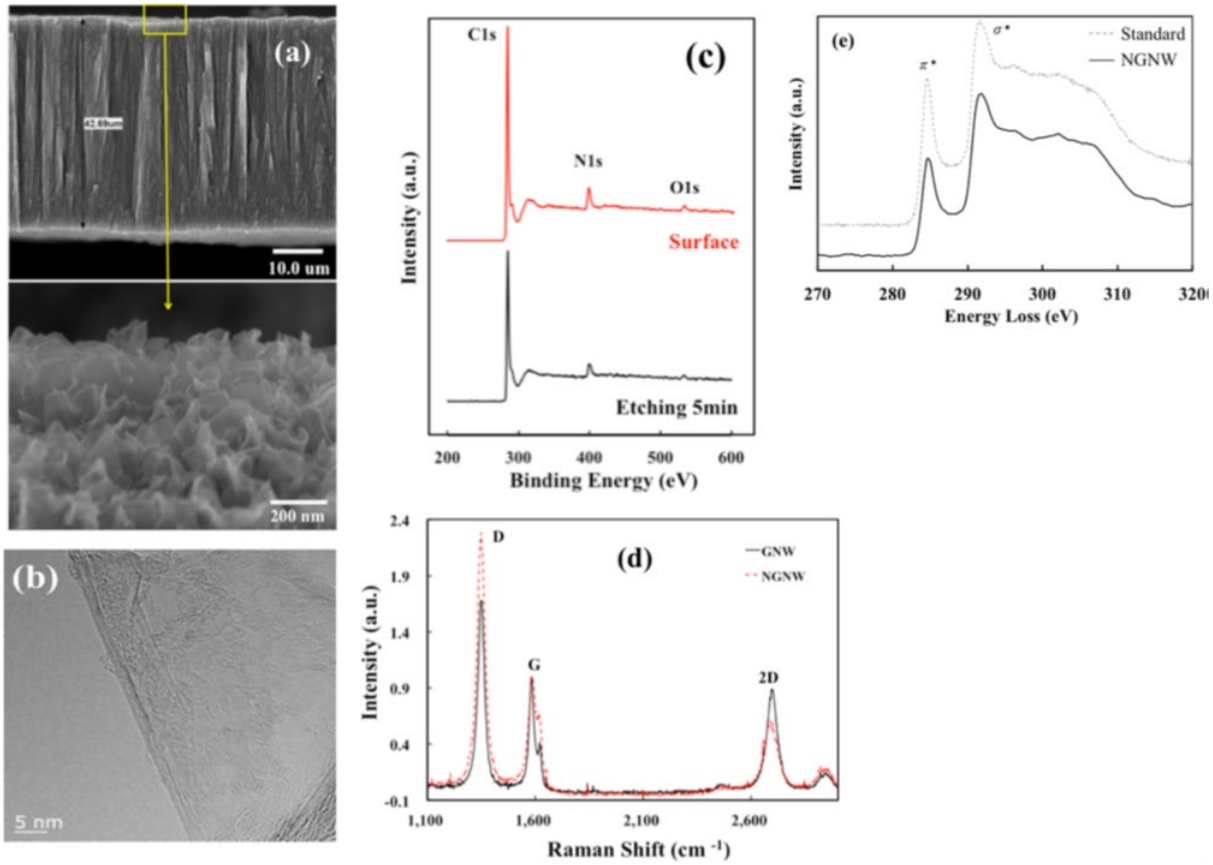

Figure 2. (a) SEM cross-section images of NGNW/Ti with a vertical structure equal to ca. 50 μm; (b) a typical STEM image of NGNW with thickness <5 atomic layers; (c) the XPS element survey spectra of NGNW (surface: as-prepared sample and the sample with 5 min plasma etching); (d) Raman spectra of GNW and NGNW; (e) EELS spectra of NGNW and graphite. Quantification of the near-edge structure indicates that the NGNW provides 93% sp^2 bonding.

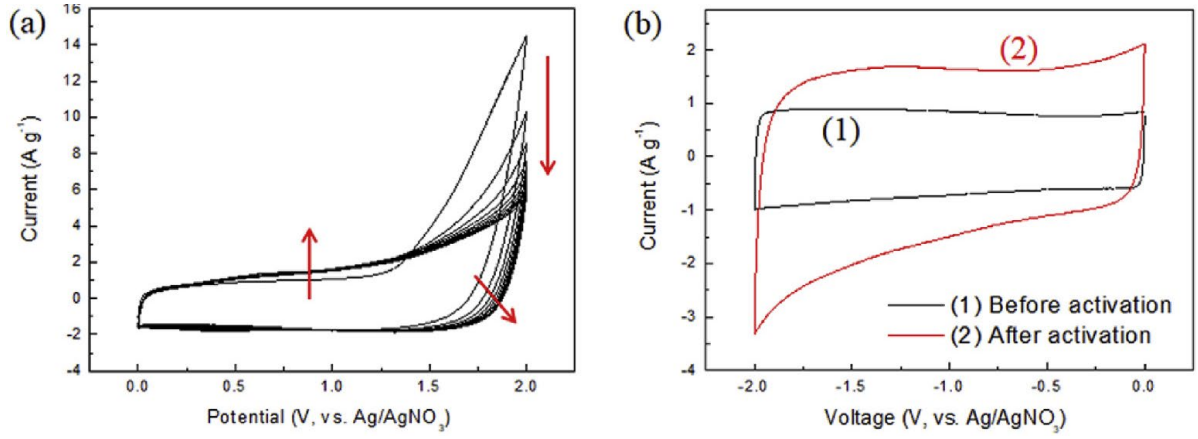

Figure 3. (a) CV curves of an as-prepared GNW/Ti electrode activated between 0 and 2 V (The direction indicated by the arrow is the change of the CV curve from the first to the tenth scan.) and (b) a comparison of CV curves before and after CV activation in 1M $TEABF_4$/PC for 10 cycles.

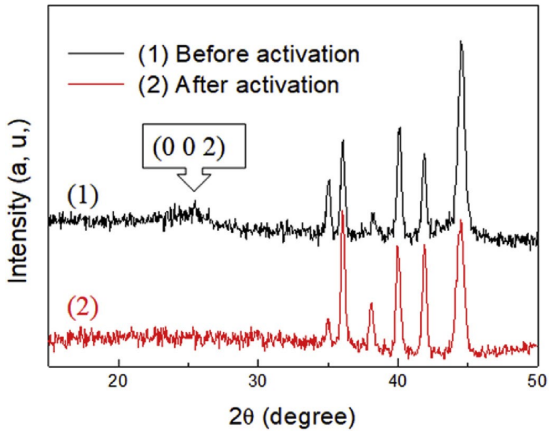

Figure 4. The GID patterns of GP60 (1) before and (2) after CV activation at 25 mV s^{-1} in 1M $TEABF_4$/PC between 0 and 2 V for 10 cycles.

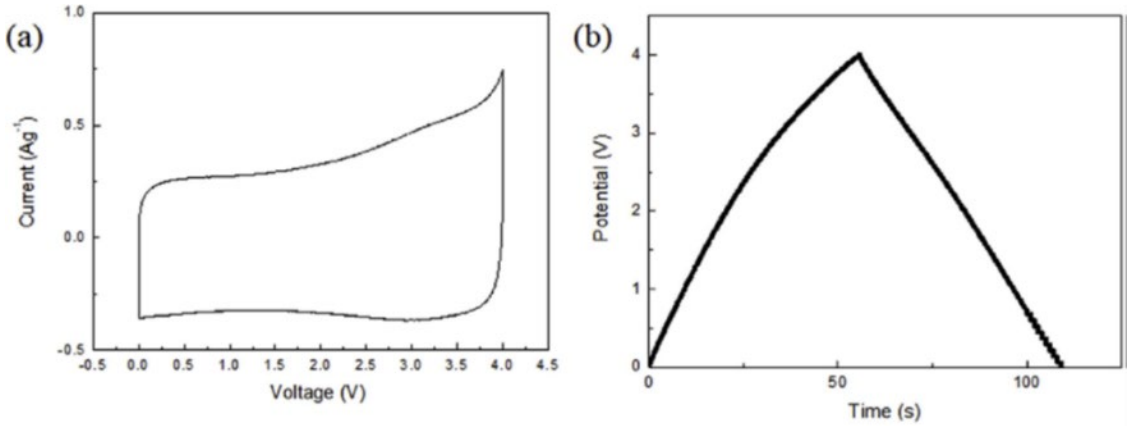

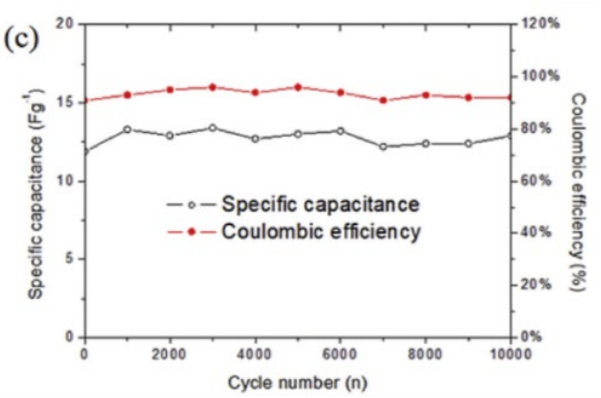

Figure 5. (a) The CV and (b) charge/discharge curves and (c) the 10,000-cycle stability test of an ASC with activated GNW and NGNW electrodes at a cell voltage of 4 V in 1M $TEABF_4$/PC.

Acknowledgments

The authors appreciate the support of Environmental Protection Administration, Executive Yuan, R.O.C. (Taiwan).

References

[1] Y. Cao, S. Tang, C. Li, P. Zhang, Y. Tan, Z. Zhang, J. Li,, *An Optimized EV Charging Model Considering TOU Price and SOC Curve*. IEEE Trans. Smart Grid 2012, 3, 388–393.

[2] Z.S. Wu, G. Zhou, L.C. Yin, W. Ren, F. Li, H.M. Cheng, *Graphene/metal oxide composite electrode materials for energy storage*, Nano Energy 2012, 1, 107-131.

[3] Y. Wang, C.X. Guo, J. Liu, T. Chen, H. Yang, C.M. Li, *CeO2nanoparticles/graphene nanocomposite-based high performance supercapacitor*, Dalton Trans. (2011) 6388-6391.

[4] H.R. Naderi, H.R. Mortaheb, A. Zolfaghari, *Supercapacitive properties of nanostructured MnO2/exfoliated graphite synthesized by ultrasonic vibration*, J. Electroanal. Chem. 719 (2014) 98-105.

[5] M. Winter, R.J. Brodd, *What Are Batteries, Fuel Cells, and Supercapacitors?*, Chem. Rev. 104 (2004) 4245-4270.

[6] A. K. Geim, K.S. Novoselov, *The rise of graphene*, Nat. Mater. 6 (2007) 183-191.

[7] Kohlschütter, P. Haenni, *Zur Kenntnis des Graphitischen Kohlenstoffs und der Graphitsäure*, Z. Anorg. Allg. Chem. 105 (1918) 121-144.

[8] G. Ruess, F. Vogt, *Höchstlamellarer Kohlenstoff aus Graphitoxyhydroxyd. Monatshefte*, Monatsh. Chem. 78 (1948) 222-242.

[9] Y.W. Zhu, S. Murali, W.W. Cai, X.S. Li, J.W. Suk, J.R. Potts, R.S. Ruoff, *Graphene and graphene oxide: synthesis, properties, and applications*, Adv. Mater.22 (2010) 3906-3924.

[10] Hsiao-Hsuan Shen, Chi-Chang Hu, *Capacitance Enhancement of Activated Carbon Modified in the Propylene Carbonate Electrolyte*, J. Electrochem. Soc. 161 (2014) 1828-1835.

[11] Hsiao-Hsuan Shen, Chi-Chang Hu, *A high-voltage asymmetric electrical double-layer capacitors using propylene carbonate*, Electrochem. Commun. 70 (2016) 23-27.

[12] Hsiao-Hsuan Shen, Chi-Chang Hu, *Determination of the upper and lower potential limits of the activated carbon/propylene carbonate system for electrical double-layer capacitors*, J. Electroanal. Chem. 779 (2016) 161-168.

[13] A. Adriano, K.C. Chun, B. Alessandra, P. Martin, *Electrochemistry of Graphene and Related Materials*,Chem. Rev. 114 (2014) 7150-7188.

[14] K.S. Novoselov, A.K. Geim, S.V. Morozov, D. Jiang, Y. Zhang, S.V. Dubonos, I.V. Grigorieva, A.A. Firsov, *Electric Field Effect in Atomically Thin Carbon Films*, Science 306 (2004) 666-669.

[15] Y. Hernandez, V. Nicolosi, M. Lotya, F.M. Blighe, Z.Y. Sun, S. De, I.T. McGovern, B. Holland, M. Byrne, Y.K. Gun'ko, J.J. Boland, P. Niraj, G. Duesberg, S. Krishnamurthy, R. Goodhue, J. Hutchison, V. Scardaci, A.C. Ferrari, J.N. Coleman, *High-yield production of graphene by liquid-phase exfoliation of graphite*, Nat. Nanotechnol. 3 (2008) 563-568.

[16] A. Jnioui, A. Metrot, A. Storck, *Electrochemical Production of Graphite Salts using a Three-Dimensional Electrode of Graphite Particles*, Electrochim. Acta 27 (1982) 1247-1252.

[17] Y. Takada, R. Fujii, *The Electrochemical Formation of Graphite Intercalation Compound in r-Butyrolactone*, Tanco Tanso 1985 (1985) 110.

[18] M. Noel, R. Santhanam, M.F. Flora, *Effect of polypyrrole film on the stability and electrochemical activity of fluoride based graphite intercalation compounds in HF media,* J. Appl. Electrochem. 24 (1994) 455-459.

[19] H. Takenaka, M. Kawaguchi, M. Lerner, N. Bartlett, *Synthesis and characterization of graphite fluorides by electrochemical fluorination in aqueous and anhydrous hydrogen fluoride*, J. Chem. Soc. Chem. Commun. (1987) 1431-1432.

[20] M. Inagaki, N. Iwashita, Z.D. Wang, Y. Maeda, *Electrochemical synthesis of graphite intercalation compounds with nickel and hydroxides*, Synth. Met. 26 (1988) 41-47.

[21] K. Ostrikov, I. Levchenko, S. Xu, *Computational plasma nanoscience: where plasma physics meets surface science*, Comput. Phys. Commun. 177 (2007) 110 – 113.

[22] I. Levchenko, O. Volotskova, A. Shashurin, Y. Raitses, K. Ostrikov, M. Keidar, *The large-scale production of graphene flakes using magnetically-enhanced arc discharge between carbon electrodes*, Carbon 48 (2010) 4570–4574.

[23] I. Levchenko, K. Ostrikov, D. Mariotti, *The production of self-organized carbon connections between Ag nanoparticles using atmospheric microplasma synthesis*, Carbon 47 (2009) 344–347.

[24] L.L. Zhao, X.Y. Liu, C.Y. Wan, X.R. Ye, F.H. Wu, *Soluble graphene nanosheets from recycled graphite of spent lithium ion batteries*, J. Mater. Eng. Perform. 27 (2018) 875–880.

[25] I.B. Denysenko, S. Xu, J.D. Long, P.P. Rutkevych, N.A. Azarenkov, K. Ostrikov, *Inductively coupled Ar/CH4/H2 plasmas for low-temperature deposition of ordered carbon nanostructures*, J. Appl. Phys. 95 (2004) 2713–2724.

[26] C. Merino, P. Soto, E. Vilaplana-Ortego, J.M. Gomez de Salazar, F. Pico, J.M. Rojo, *Carbon nanofibres and activated carbon nanofibres as electrodes in supercapacitors*, Carbon 43 (2005) 551–557.

[27] Hsiang-Feng Yen, Ying-Ying Horng, Ming-Shien Hu, Wei-Hsun Yang, Je-Ruei Wen, Abhijit Ganguly, Yian Tai, Kuei-Hsien Chen, Li-Chyong Chen, *Vertically aligned epitaxial graphene nanowalls with dominated nitrogen doping for superior supercapacitors*, Carbon, 2015, 82, 124-134.

[28] Jinhua Li, Minjie Zhu, Zhuqing Wang, and Takahito Ono, *Engineering micro-supercapacitors of graphene nanowalls/Ni heterostructure based on microfabrication technology*, Appl. Phys. Lett. 2016, 109, 1539011-1539015.

[29] Yu-Wen Chi, Chi-Chang Hu, Hsiao-Hsuan Shen, and Kun-Ping Huang, *New Approach for High-Voltage Electrical Double-Layer Capacitors Using Vertical Graphene Nanowalls with and without Nitrogen Doping*, Nano Lett. 2016, 16, 5719−5727.

[30] Jinhua Li, Minjie Zhu, Zhonglie An, , Zhuqing Wang, Masaya Toda, Takahito Ono, *Constructing in-chip micro-supercapacitors of 3D graphene nanowall/ruthenium oxides electrode through silicon-based microfabrication technique*, J. Power Sources, 2018, 401, 204-212.

[31] Da-Je Hsu, Yu-Wen Chi, Kun-Ping Huang, Chi-Chang Hu, *Electrochemical activation of vertically grown graphene nanowalls synthesized by plasma-enhanced chemical vapor deposition for high-voltage supercapacitors*, Electrochim. Acta, 2019, 300, 324-332.

[32] B. MacDougall, C. Bock, E. Gileadi, S. Gottesfeld, J. Leddy, B. Scrosati, S. Trasatti, S. Morin, *Electrochemistry: Symposium on Interfacial Electrochemistry in Honor of Brian E. Conway*, ECS Trans. 25 (2010) 15-23.

[33] Ferrari A C, Tanner B K, Stolojan V, Brown L M, Rodil S E, Kleinsorge B, and Robertson J, *Density, sp3 fraction, and cross-sectional structure of amorphous carbon films determined by X-ray reflectivity and electron-energy-loss spectroscopy*. Phys. Rev. B 62 (2000) 11089–11103

[34] Jing-Yi Yan, Fu-Rong Chen and Ji-Jung Kai, *Mapping of sp2/sp3 in DLC thin film by signal processed ESI series energy-loss image*, Journal of Electron Microscopy 51 (2002) 391–400

[35] Jiayuan Li, Xinghua Li, Penghui Zhao, Dang Yuan Lei, Weilong Li, Jintao Bai, Zhaoyu Ren, Xinlong Xu, *Searching for magnetism in pyrrolic N-doped graphene synthesized via hydrothermal reaction*, CARBON 84 (2015) 460 – 468

[36] Tianyu Liu, Cheng Zhu, Tianyi Kou, Marcus A. Worsley, Fang Qian, Cecilia Condes, Eric B. Duoss, Christopher M. Spadaccini, Yat Li, *Ion Intercalation Induced Capacitance Improvement for Graphene-Based Supercapacitor Electrodes*, Chem. Nano. Mat. 2 (2016) 635-641.

Author

Kun-Ping Huang obtained his Ph.D. in Department of Material Science and Engineering from National Chiao Tung University in 2004. Before that, he worked in Advanced Module Department of tsmc R&D as a principle engineer starting from 2003. In 2008, he transferred to Mechanical and Systems Research Laboratories, ITRI, as a researcher. His research focuses on graphene related materials, including the fundamental study on doped graphene, and industry-scale production and the applications. He also works on microwave annealing for semiconductor, solar cell and carbon fiber annealing process developments.